RSC Advances

PAPER

View Article Online
View Journal | View Issue

Cite this: *RSC Adv.*, 2024, **14**, 31451

Development of eco-friendly pretreatment processes for high-purity silicon recovery from end-of-life photovoltaic modules†

Suhwan Kim, ‡[a] Junkee Kim,‡[bc] Seyeon Cho,[a] Kwangmin Seo,[b] Byoung-Uk Park,[d] Hae-Seok Lee[c] and Jongsung Park *[a]

Received 6th July 2024
Accepted 27th September 2024

DOI: 10.1039/d4ra04878d

rsc.li/rsc-advances

This study examines the efficacy of photovoltaic (PV) recycling processes and technologies for the recovery of high-purity silicon powder from waste solar modules. In order to facilitate the simplification of complex processes, such as the conventional nitric acid dissolution, solvent and ultrasonic irradiation, and solvent dissolution, a variety of mechanical separation processes have been established. These processes are designed to enhance the efficiency and effectiveness of the aforementioned processes. And a novel method for separating EVA from recycled Si powder was devised, which studied the WGS process using aqueous solutions of H_2O, HNO_3, and NaCl with different specific gravities. The WGS process using NaCl solution demonstrated superior performance, removing over 94% of the EVA, requiring less energy input and producing 73% less CO_2 emissions compared to the thermal process. These technologies facilitate the transition towards a circular economy and bolster the implementation of carbon-neutral initiatives.

1. Introduction

The world strives to achieve a carbon-neutral society in response to the climate change crisis and to fulfill the common goals of realizing a sustainable society (SDGs) while preserving the Earth's ecosystem (biodiversity conservation).[1–3] Green technologies can solve global issues such as carbon neutrality, net zero, and the circular economy. Proactive environmental management technologies benefit human society and the natural environment.[4,5] They are essential to solve future environmental problems beyond the current post-processing environmental problems. The development of genuinely carbon-neutral green technologies is required to transition from an existing advanced economy to a circular economy. Efforts to minimize the environmental impact of the technology application process are urgently needed.[6–8]

Green climate technologies help mitigate climate change and promote sustainable development. These technologies include renewable energy technologies such as solar, wind, hydropower, and sustainable energy sources without greenhouse gas emissions.[9,10] In particular, solar technology is a renewable energy source that does not deplete natural resources. It is an essential component of carbon-neutral policies to reduce carbon emissions and mitigate climate change.[11,12] Additionally, it is cost-effective, accessible, and reliable for resilient and sustainable energy systems. It generates electricity without emitting greenhouse gases or other harmful pollutants, reducing carbon emissions and mitigating the effects of climate change.[13–15] This corresponds to the core technology at net zero. Existing solar panel recycling technologies use simple landfills,[16] pyrolysis,[17,18] chemical processes,[19,20] and physical methods[21–23] known as universal recycling and reuse methods. These technologies involve crushing or pulverizing panels while dismantling the frame and junction box, retaining the glass, and sorting them into individual materials. This results in low economic feasibility because all constituent materials are mixed.[24,25]

This study employs a circular economy-compatible and eco-friendly physical method, which separates the remaining glass from the panel after dismantling the aluminum frame and junction box, as well as the sandwich (encapsulating material) that connects them. This method, unlike general crushing methods, allows for the recovery of glass with high purity (95%) and can ensure the production efficiency of recycled materials.

However, using a recycling method that allows the recovery of raw materials by selecting valuable metals, such as silicon, copper, and silver, presents a challenge. Micronized glass and encapsulating materials such as ethylene vinyl acetate (EVA) are mixed after the crushing or grinding. Moreover, with the

[a]*Department of Energy Engineering, Future Convergence Technology Research Institute, Gyeongsang National University, Jinju, Gyeongsangnam-do 52828, Republic of Korea. E-mail: j.park@gnu.ac.kr*

[b]*WonKwang S&T Co., Ltd, Incheon 22845, Republic of Korea*

[c]*Graduate School of Energy and Environment (KU-KIST Green School), Korea University, Seoul 02841, Republic of Korea*

[d]*Chungbuk Technopark, Next Generation Energy Center, Cheongju, Chuncheongbuk-do 28116, Republic of Korea*

† Electronic supplementary information (ESI) available. See DOI: https://doi.org/10.1039/d4ra04878d

‡ These authors contributed equally.

development of solar cells and module technologies that prioritize power generation efficiency, bifacial modules (G2G) and BIPV modules are gaining[26,27] market share, along with advanced Si solar cells such as PERC, TOPCon, and HIT cell technologies.[28,29] Due to this paradigm, further development of solar recycling technology requires supplementation and changes in new processes and technologies for large-scale processing and production. Glass separation technology is considered the most important in recycling existing screen-printed PV modules. Additionally, encapsulant removal or sorting technology, including EVA, must be upgraded during the crushing, grinding, and sorting processes.

The conventional approach to separating EVA from waste PV panels has been through the use of chemical and delamination methods, primarily involving the combustion of the EVA to facilitate its removal. The chemical methods employed include solvent and ultrasonic irradiation,[30] solvent dissolution,[31] and chemical etching.[32] Additionally, electrothermal heating[33] and pyrolysis techniques[34] have been explored as potential avenues for EVA removal through combustion. Nevertheless, these conventional techniques are either exceedingly time-consuming or inherently flawed due to their tendency to generate deleterious emissions and waste products. Therefore, it is imperative to develop new technologies that are comparatively more rapid than existing processes and which minimize the emission of harmful substances and carbon dioxide.

In this study, two processes were employed to remove EVA from reclaimed Si powder: thermal and wet gravity separation (WGS). The thermal process eliminates polymer components like EVA but consumes high energy and emits CO_2 emissions. The wet gravity separation process uses an aqueous NaCl solution to exploit the specific gravity difference between silicon and EVA, resulting in efficient separation. The WGS process employs the specific gravities of the materials to be separated to facilitate their centrifugation. As a consequence, it is a technology that can effectively separate EVA from reclaimed Si powder with minimal chemical usage and the generation of minimal harmful substances. This was verified using TGA, FT-IR, and SEM/EDS measurements. The CO_2 emission amounts of the two processes were also calculated.

2. Experimental section

2.1. Recycling of EoL PV modules

The entire process for recycling and reclaiming Si powder from end-of-life (EoL) PV modules is shown in Fig. 1. The details of each process are listed in Table 1. First, an automatic machine separated the aluminum frame, electrical wires, and junction box from the PV module. Then, the back sheet on the rear side

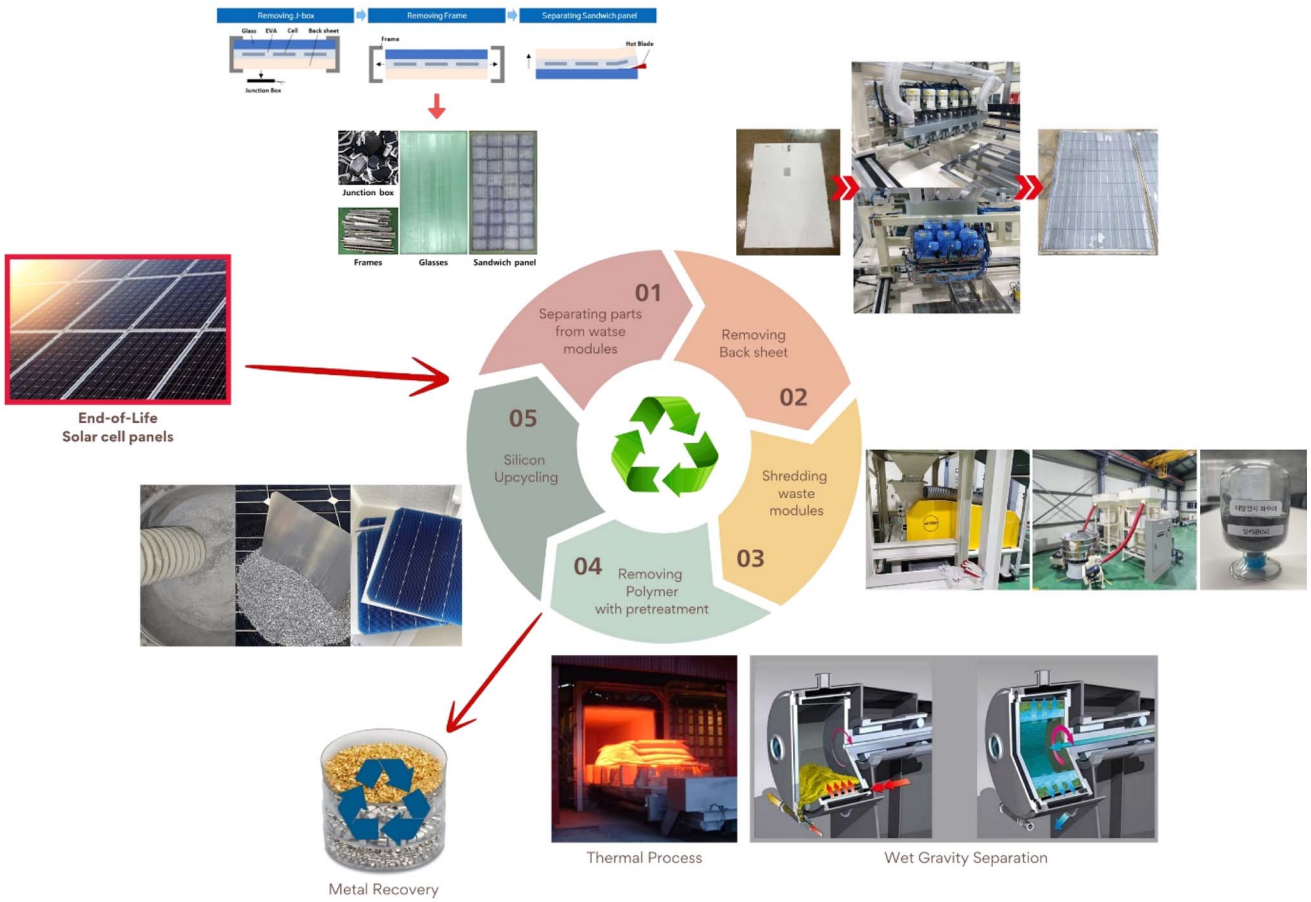

Fig. 1 Schematic diagram of the Si powder upcycling process for EoL PV modules.

Table 1 Process overview and details for PV recycling and reclaiming Si powder

Process	Schematic	Technical details
Dismantling process	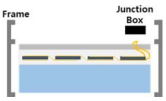	The process of dismantling the aluminum frame that protects the solar panel from external shock and the junction box that connects the electrodes to the outside Separate the frame by pushing it out from inside the module using a hydraulic press jig and remove the junction box using a blade
Sealant removal process	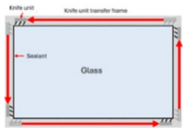	A process to remove the sealant that bonds the panel and frame as a pre-treatment process for the separation process To prevent damage during the subsequent process due to the sealant attached to the windshield, remove it by cutting it using three blades at different angles
Backsheet removal (grinding) process	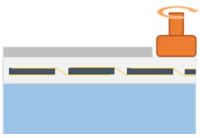	A grinding process removes the back sheet on the back side of PV modules by a grinding machine
Glass separation process	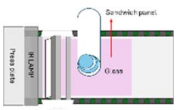	A partial heating process that separates the remaining layers (EVA/Si solar cell/EVA layers) except the front glass of the solar panel with a blade Enter the heated blade into the interface between the glass and EVA and cut
Crushing process	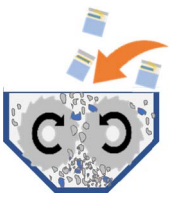	A shredding process to select solar cells encapsulated in EVA and valuable materials within the module by inserting the separated module sandwich into a rotary cutter mill Samples are crushed between the rotational speed and high precision of the rotary cutter mill Different crushing shapes are derived using differences in the physical properties of module constituent materials
Sorting process (particle separation)	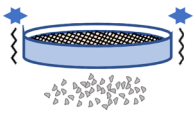	Sorting process using particle size differences in shredded materials Separating small particle size powder-type solar cells and metals (copper ribbon + solar cells in powder foam + EVA)
Sorting process (specific gravity separation)	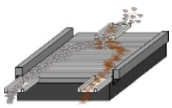	By vibration + air blow, materials with light specific gravity are affected by the air blow, and materials with heavy specific gravity (copper ribbon) are selected by the vibration
Wet gravity separation		The thermal process eliminates the EVA contained in Si powder through heat energy Wet gravity separation separates EVA contained in Si powder by specific gravity differences in various solutions

of the PV modules was ground using a mechanical grinder to make the following recycling process more accessible. A hot blade, *i.e.*, a specially built machine with a T-blade, was employed to separate the cover glass and solar cells. After this process, the Si solar cells remained attached to the EVA. In the hot-blade process, six hot knives were inserted between the cover glass and EVA/Si solar cells to achieve EVA-attached Si solar cells. Then, the Si solar cells with EVA were shredded using an in-house shredding machine, converting them to powder. To recover high-purity Si, thermal and wet gravity separation (WGS) processes were employed to remove the remaining shredded EVA mixed with Si powder.

Thermal processing was performed to remove the shredded EVA from the reclaimed Si powder. The EVA was fully carbonized at around 500 °C. Hence, the thermal process temperature was approximately 10% higher at 550 °C. The thermal process was executed at a ramp rate of 10 °C min^{-1} using a furnace. WGS was performed as follows: reclaimed Si powder (0.5 g) was mixed with 13 ml of D. I. water, HNO_3, and a 15 wt% NaCl aqueous solution. After centrifugation at different revolutions per minute (RPM) for various times, the separated components were allowed to float to the top for 10 min. The material floating in the upper layer was discarded, and the settled material was washed with D. I. water and dried.

2.2. Characterization of separation processes

A thermogravimetric analyzer (TGA, TGA N-1000, SCINCO) was used to evaluate the thermolysis characteristics of the samples in a nitrogen atmosphere at a temperature increase rate of 10 °

C min^{-1}. To identify polymers or other organic components remaining in the samples before and after pretreatment, Fourier transform infrared (FT-IR, US/Spectrum to FT-IR, PerkinElmer) measurements were made at 500–4000 cm^{-1}, and Raman spectroscopy (i-Raman Plus, BW TEK) was performed at 250–300 cm^{-1} equipped with a laser at a wavelength of 532 nm and a fiber optic probe. The crystallinity of the thermal or WGS powder was examined by X-ray diffraction (XRD, Ultima IV, Rigaku), field-emission scanning electron microscopy (FE-SEM), and energy dispersive spectroscopy (EDS, MIRA3 LM, TESCAN) to determine the morphology and composition ratios of the metal components.

3. Results and discussion

3.1. Reclaiming of Si powder from EoL PV modules

The aluminum (Al) frame and junction box were first removed to recycle the PV modules and reclaim Si in powder form, as described in Table 1, and this is a simple method that uses automated equipment. After removing the junction box and Al frame, the PV modules (Fig. 2(a)) were placed in the equipment (Fig. 2(b)) for back-sheet removal. The back-sheet removal equipment consisted of a module transfer unit and a three-stage back-sheet removal unit. The back-sheet was ground using six T-cutters arranged in a zigzag arrangement (Fig. 2(c)), and these T-cutters grinded polymeric back sheet. The PV module processed by back removal is shown in Fig. 2(d). The process was carefully controlled to only grind back sheet layer, and not grind Si solar cells. The figure shows that the back-sheet attached to the PV modules was almost completely removed during this process, and the Si solar cell was not grinded by the process. This is because the purpose of the recycling processes is reclaiming Si for EoL module, so that Si loss by this process must be minimized. Also, this process has another advantageous that it prevents TiO_2 particles contained back sheet for following Si reclaiming process, and allows the recovery of high-purity silicon powder. Hence, it needs to be removed in advance.

The next step was separating the front cover glass and the Si solar cells (Fig. 3(a)). For this, a hot-knife process was employed. In the hot-blade process, six hot knives were inserted between the cover glass and EVA/Si solar cells, resulting in EVA-attached Si solar cells after the process and the front cover glass in full, as shown in Fig. 3(b). The front glass and Si solar cells with EVA were successfully separated through this process, facilitating the curled Si solar cells as shown in Fig. 3(b). This process is advantageous because it generates significantly less CO_2 than the thermal annealing process, which applies heat to whole PV panels to burn the EVA layer to separate Si solar cells and the front glass. Subsequently, the curled Si solar cells were crushed by a rotary cutter mill cuts and crushes the Si solar cells into powder (Fig. 3(c)). Finally, vibration and air blowing process were conducted to separate Cu ribbon scrap and light weight Si powder as shown in Fig. 3(d). Through these processes, Si powder was successfully obtained from the EoL PV modules. It can be claimed that these processes are composed of fewer carbon emission processes and efficiently recycle large amounts of EoL PV modules to achieve a circular economy and carbon neutrality.

Following these processes, the as-reclaimed Si powder containing shredded EVA was obtained. As mentioned earlier, minimizing polymeric impurities in Si powder is crucial to using it as a base material for high-value upcycled products such as SiC or SiN_x. For this purpose, the amount of polymer EVA in the as-reclaimed Si powder was analyzed after shredding and separation using TGA, FT-IR, SEM, and EDS. As shown in the TGA analysis results in Fig. 4(a), the reclaimed Si powder exhibited mass loss in two regions at 265–400 and 400–500 °C,

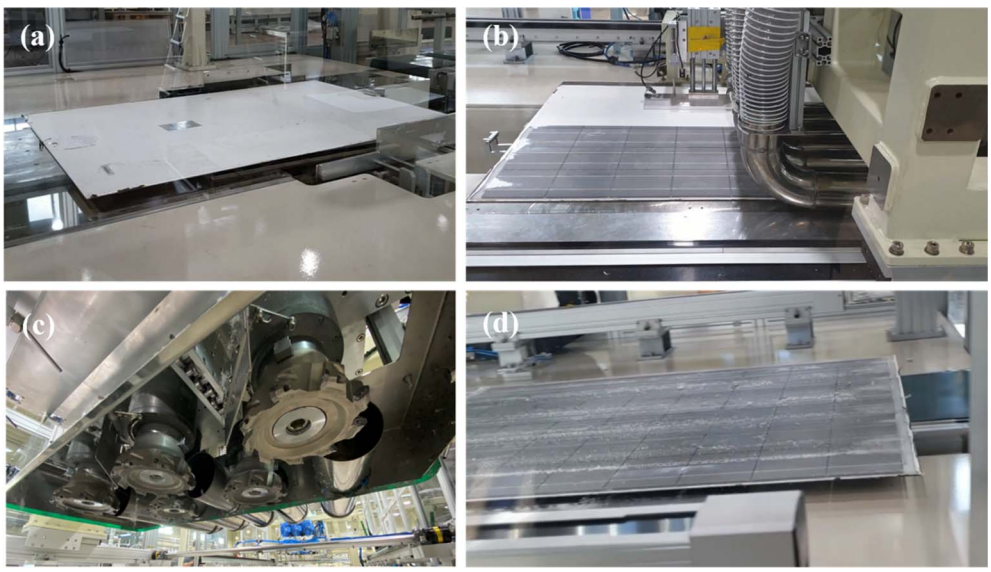

Fig. 2 Process overview of the back-sheet, (a) Al flame and junction box removed PV module, (b) automatic transfer PV modules, (c) image of T-cutter of the back-sheet removal equipment and (d) PV module after back-sheet removal process.

Fig. 3 Process overview of hot-knife, crushing, and sorting, (a) hot-knife equipment, (b) recovered front cover glass and curled Si solar cells after the hot-knife process, (c) crushing and sorting process, and (d) final products after whole recycling processes.

which showed the same weight loss pattern of EVA as in our previous report.[21] The percentages of mass loss in each region were respectively 6.1% and 21.8% for a total mass loss of 27.9%. The reclaimed Si powder contained approximately 27.9% polymer components. No further mass loss was observed at temperatures above 500 °C. FT-IR measurements of the reclaimed Si powder showed various stretching bonds with oxygen or hydrogen, confirming the presence of polymeric

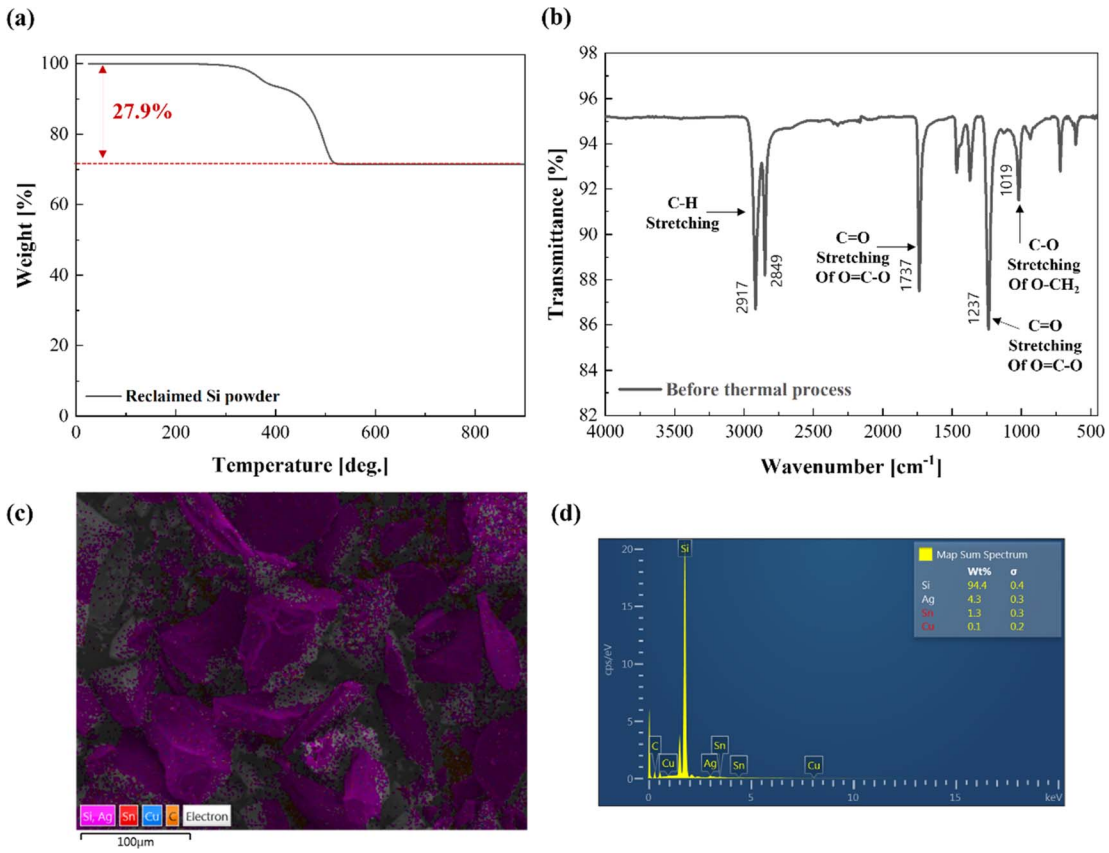

Fig. 4 (a) TGA, (b) FT-IR, (c) SEM, and (d) EDS measurement results of reclaimed Si powder.

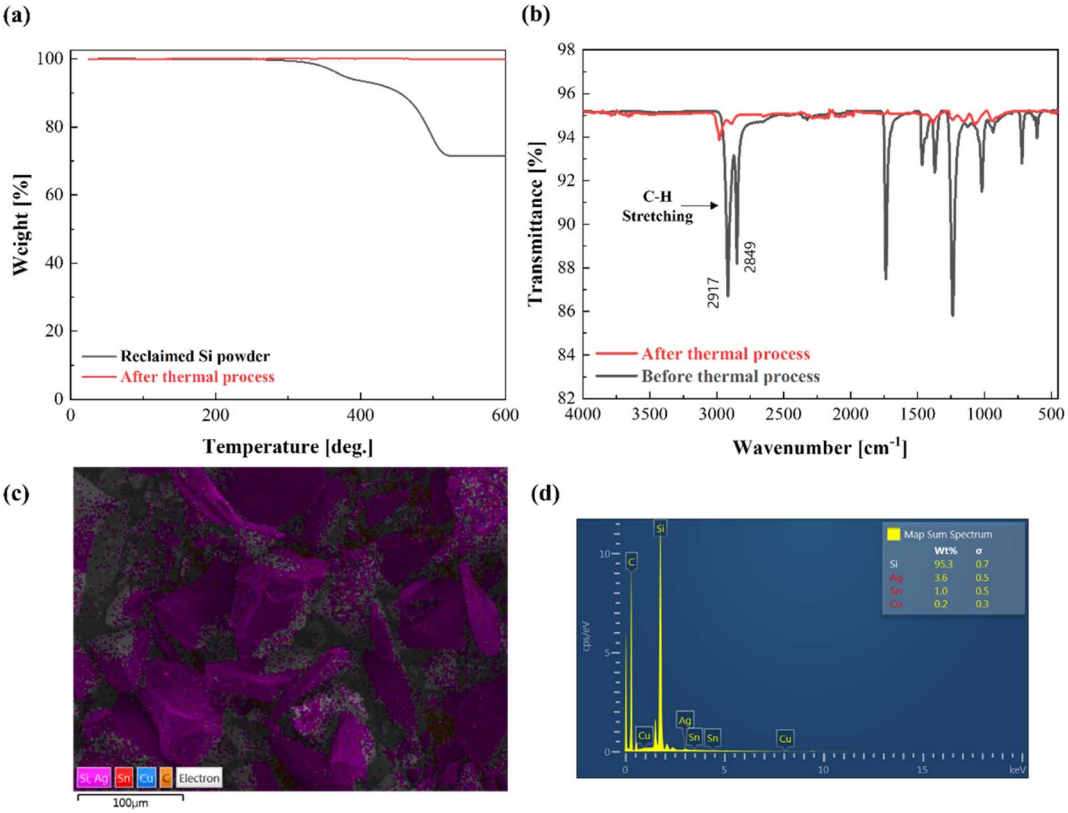

Fig. 5 (a) TGA, (b) FT-IR, (c) SEM, and (d) EDS measurement results of reclaimed Si powder after the thermal process.

components (Fig. 4(b)). SEM/EDS measurements confirmed that the Si content was greater than 94 wt%, followed by Ag, Sn, and Cu. However, in the case of Cu, the content was the lowest because it had already separated into Cu ribbons during the reclamation of the Si powder (Fig. 4(c and d)). These metals can be removed by leaching in the HNO_3 process. Therefore, removing Ag, Sn, and Cu is not discussed further.

3.2. Thermal process

In this study, two processes were employed to remove the shredded EVA from the reclaimed Si powder: (i) thermal and (ii) wet gravity separation (WGS). First, a thermal process was employed to remove the shredded EVA from the reclaimed Si powder. The initial assessment found that EVA was fully carbonized at around 500 °C, as shown in Fig. 4(a). Thus, the thermal process was conducted at a slightly higher temperature of 550 °C for 10 min in air to remove EVA efficiently. Thermal processing eliminates polymers through heating, which is simple and does not require specialized equipment. However, it has disadvantages, including the need for thermal energy input for heating and the generation of CO_2 due to polymer carbonization.

Fig. 5 shows the characteristics of the reclaimed Si powder after thermal processing. The TGA analysis in Fig. 5(a) indicates no mass loss, thus suggesting 100% polymer removal through the thermal process at 550 °C for 10 minutes. FT-IR, Raman spectroscopy, XRD, SEM, and EDS analyses were conducted to corroborate the results of the polymer removal by thermal processing. FT-IR measurements showed that other than the two C–H stretching vibration peaks in the range of 2850–2950 cm^{-1} (Fig. 5(b)), which can be found on a typical Si wafer or silica, other organic peaks were almost eliminated.[35,36] Scanning electron microscopy (SEM) and energy-dispersive X-ray spectroscopy (EDS) measurements after the thermal process showed no significant change in the existing metal content (Fig. 5(c and d)). The prominent peaks of Si, which accounted for the most significant proportion, were confirmed by the XRD results (Fig. S1(a)†). Therefore, the thermal process efficiently removed the shredded EVA in the Si powder by applying heat.

3.3. Wet gravity separation

Second, the WGS process was employed to remove the shredded EVA from the reclaimed Si powder effectively. The wet process typically refers to acid leaching, which initially extracts the target metal from the ore into the ionic phase (dissolution) and is followed by precipitation and reduction. The WGS process has the advantage of not requiring a thermal budget compared to the thermal process and minimizing the amount of carbon dioxide produced.[37] The WGS process was designed using the difference in the specific gravity of EVA, which accounted for the highest proportion of polymer components and Si. Considering that Si and EVA have specific gravities of 2.42 and 0.9,[38,39] using a solution with a specific gravity value between the two

Table 2 Specific gravity values of Si, EVA, and solutions used for specific gravity separation

				NaCl solution		
	Si	EVA	H_2O	10 wt%	15 wt%	HNO_3 (60%)
Specific gravity	2.42	0.9	0.99	1.072	1.107	1.37

materials would have caused Si to sink. EVA would float to the top and could be separated after centrifugation. Therefore, the reclaimed Si powder was mixed in liquids of different specific gravities and separated using centrifugation. Three different liquids were employed: H_2O with a specific gravity of 0.99, HNO_3 (60%) with a specific gravity of 1.37, and an aqueous solution of NaCl (10 and 15 wt%) with a specific gravity of 1.072 and 1.107 as listed in Table 2. H_2O was chosen because it does not pollute the environment, does not react with other substances in the silicone powder, and is easy to dispose. The subsequent consideration of NaCl solution was prompted by its potential to enhance the specific gravity of H_2O while exhibiting no anticipated reactivity with Sn, Ag, and Cu in the solar cell. The utilization of HNO_3 was ultimately deemed appropriate due to its ability to dissolve and separate the metals.

Fig. 6 illustrates the characteristics of the Si powder after WGS with different solutions at 5000 rpm for 10 min. First, TGA measurements were conducted to determine the weight loss of the reclaimed Si powder after WGS using different solutions. As observed in Fig. 6(a), in the case of deionized (D. I.) water alone, the decrease in mass occurred in the temperature range of 330, 420, and 500 °C, with a total reduction of approximately 20% compared to the reclaimed Si powder without the WGS process. The results obtained using D. I. water did not show significant separation performance.

In the WGS process using nitric acid, the polymer or residual metal components were dissolved in nitric acid and precipitated together, resulting in poor separation capability. The total mass reduction increased by more than 4% compared to the reclaimed Si powder. In particular, the mass reduction in the relatively high-temperature range of 380–500 °C increased by approximately 8%, resulting in a total mass loss of 32.5%. Using a 15 wt% aqueous solution of NaCl, the mass loss was approximately 0.5% up to 450 °C and ~3.4% between 450 and 500 °C. The total mass loss was 3.8%, indicating that the residual polymer components were successfully separated (Table S1†).

FT-IR measurements after the wet separation pretreatment agreed with the TGA results and showed that the NaCl aqueous solution resulted in the most significant decrease in other organic transmittance values below 2750 cm^{-1} (Fig. 6(b)). Raman spectroscopy measurements revealed no peaks other than the Si–O–Si peak at 515–520 cm^{-1} and the Si–OH peak at 900–970 cm^{-1}.[40] In the case of HNO_3, the peaks broadened and sharpened because of poor separation. The poor separation performance of HNO_3 was also confirmed by Raman spectroscopy measurements, as evidenced by the NO_3^- symmetry stretch at 1052 cm^{-1} (Fig. 6(c)).

From the results of XRD after the WGS process, dominant peaks of Si were confirmed in the samples using DI water and NaCl aqueous solutions, similar to the thermal process. However, when HNO_3 was used, the separation did not occur properly, and many minor peaks were observed below 55 °C (Fig. S1(b)†). The EDS measurement results showed a trend similar to the separation performance. When HNO_3 was used, the Ag, Sn, and Cu contents were higher than when other solutions were used, compared to the Si content. It is presumed that the separation occurred when the metal components were dissolved and settled in the nitric acid. When D. I. water and NaCl aqueous solutions were used, the Si content was over 98%, confirming high separation performance (Fig. S2†).

Based on these results, the optimal conditions using aqueous NaCl solution were investigated. To optimize the process, the concentration of the NaCl aqueous solution was reduced to determine whether the number of chemicals could be further reduced, and the centrifuge rotation speed and rotation time were adjusted.

In Fig. 7 and Table 3, TGA measurements showed that the centrifugation speed and time were higher for a higher concentration of NaCl aqueous solution, and better separation results were achieved. For the 10% NaCl aqueous solution, the 4000 rpm condition showed a considerable variation in the total weight loss values with rotation time. The 4000 rpm–10 min condition showed slight separation compared to the reclaimed Si powder. The 5000 rpm–10 min condition showed the best

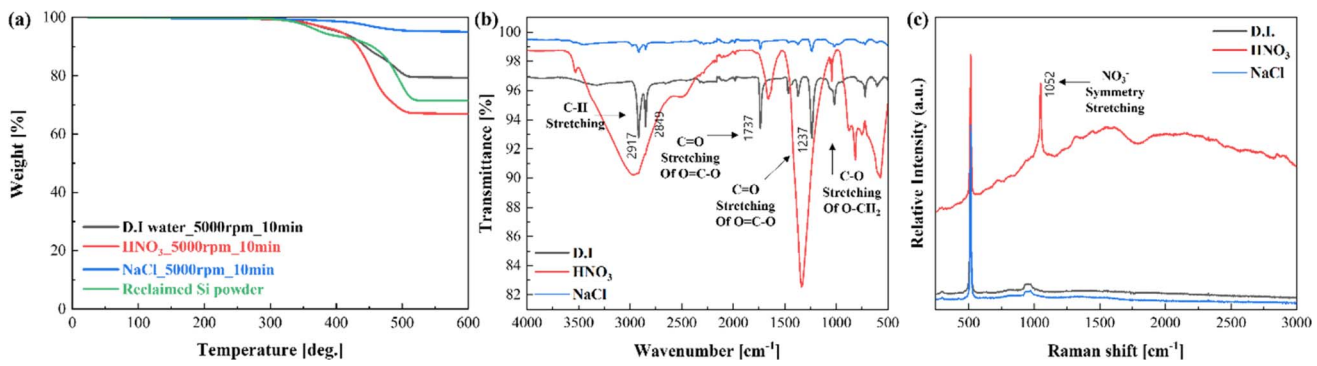

Fig. 6 Results of (a) TGA, (b) FT-IR, and (c) Raman spectroscopy measurements of reclaimed Si powder after the WSG process using different solutions.

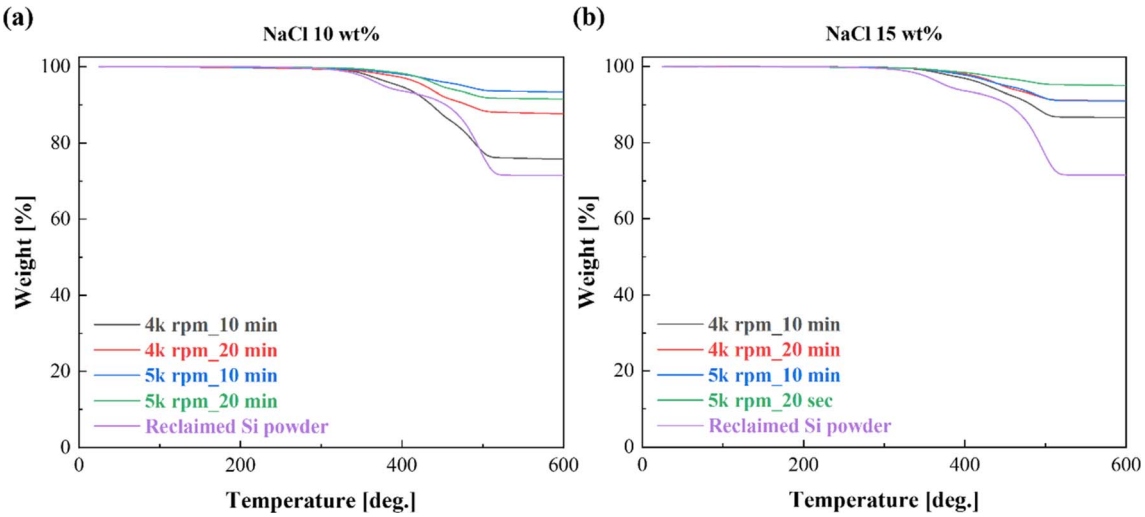

Fig. 7 TGA results after wet separation pretreatment with aqueous NaCl solutions at concentrations of (a) 10 and (b) 15 wt%.

Table 3 Weight loss temperature and percentage according to the concentration of NaCl aqueous solution and centrifugation speed and time

		Weight loss temperature (°C) and percentage			
Experimental condition	Weight (mg)	Total	1st	2nd	3rd
NaCl 10 wt% 4k rpm_10 min	10.686	23.298%	271.9–389 (3.937%)	389–460 (9.635%)	460.6–524.1 (9.726%)
NaCl 10 wt% 4k rpm_20 min	10.422	11.052%	297.9–462.6 (8.061%)		466.6–521.5 (2.991%)
NaCl 10 wt% 5k rpm_10 min	10.256	5.444%	304.6–378.8 (0.999%)	391.7–453.2 (2.124%)	457.2–515.3 (2.321%)
NaCl 10 wt% 5k rpm_20 min	10.826	8.001%		306.7–526.2 (8.001%)	
NaCl 15 wt% 4k rpm_10 min	11.1	12.395%	297.3–383.5 (2.162%)	389.7–457.3 (4.885%)	461.9–525.4 (5.348%)
NaCl 15 wt% 4k rpm_20 min	10.878	8.424%	312–464.7 (2.527%)		465.8–527.4 (5.897%)
NaCl 15 wt% 5k rpm_10 min	**10.907**	**3.808%**	**307.3–450.4 (0.465%)**		**451.5–513.3 (3.343%)**
NaCl 15 wt% 5k rpm_20 min	10.786	4.322%	305.2–453.1 (1.529%)		455.8–514.0 (2.793%)
Reclaimed Si powder	18.29	27.936%	265.0–399.1 (6.112%)		408.7–540.3 (21.824%)

Table 4 A comparison of the generation of CO_2 in thermal *versus* WGS process

	Usage amount	CO_2 emission factor (kg CO_2 per kg)	Thermal process CO_2 generation	WGS process CO_2 generation
Water (5000 rpm, 10 m)	24.19 L	0.01	—	0.24
NaCl solution (15 wt%)	3.63 kg	0.06	—	0.21
Centrifugation (5000 rpm, 10 m)	19 kW h	0.5	—	9.5
Thermal process (550 °C)	55 kW h	0.5	27.5	—
Total (kg CO_2 per kg)			27.5	9.95

separation performance of 5.4%. The 15 wt% NaCl aqueous solution showed a weight loss difference of more than 10% even at 4000 rpm–10 min compared to the 10 wt% solution. Similar to the results for the 10 wt% NaCl aqueous solution, the best weight loss of 3.8% was obtained at 5000 rpm for 10 min. Even with a slight difference of 0.1 in the specific gravity between the two solutions, separation performance varied significantly.

Hence, the results differed depending on the rotation time at relatively low rotation speeds. Analyzing the overall trend, the wt% of NaCl and the rotation speed are more significant factors than the rotation time. This trend suggests that aqueous solutions with sufficient specific gravity differences and rotational speeds are required to separate the attached or mixed polymers from the reclaimed Si powder. In particular, the EVA adhering more closely to the cell requires more centrifugal force for removal. These results demonstrate the suitability of the WGS process for effectively separating EVA from the reclaimed Si powder.

Table 4 compares the carbon emissions generated to assess the relative efficiency of the thermal process, and WGS developed in this study. The thermal process involved heat treatment up to 550 °C in a conventional small furnace, whereas the wet

process was based on centrifugation using a 15 wt% aqueous solution of NaCl. For both processes, the power and material volumes were calculated based on the processing of 1 kg of recycled silicone powder, as shown in Table 4. The CO_2 emissions from pretreatment with 1 kg of recycled silicone powder were approximately 27.5 kg CO_2 per kg for the thermal process and 10 kg CO_2 per kg for the WGS process. The thermal process emitted 2.75 times more carbon dioxide than the WGS process. Moreover, NaCl is not hazardous to humans or the environment and does not require specific wastewater treatment. Therefore, it can be concluded that using NaCl solution to treat the reclaimed Si powder is a highly environmentally friendly and efficient process.

4. Conclusion

This study established an efficient PV recycling process, and a WGS process for reclaimed Si powders was developed. After recycling, the EoL PV modules were successfully treated, and the reclaimed Si powder was retained for future upcycling. This study also successfully demonstrated the viability of reclaiming high-purity silicon powder from solar cell waste modules using thermal and WGS processes. The thermal process at 550 °C effectively removed all polymer components, specifically EVA, from the reclaimed silicon powder, as confirmed by various analytical techniques such as TGA, FT-IR, SEM, and EDS. While effective, the thermal process has notable drawbacks, including high energy consumption and significant carbon dioxide emissions, making it less environmentally friendly than the WGS.

The WGS process was evaluated as an effective method for recycling Si powder from EoL PV modules, focusing on removing EVA and other polymer components. The process was tested using DI water, HNO_3, and a 15 wt% aqueous solution of NaCl, with the NaCl solution demonstrating the highest separation efficiency. TGA showed a total mass loss of only 3.8% using the NaCl aqueous solution through process optimization, indicating the successful removal of more than 96% of the EVA. FT-IR and Raman spectroscopy analyses confirmed the high efficiency of the NaCl solution in reducing polymers from the reclaimed Si powder. These analyses indicate a significant reduction in the organic peaks, confirming the effective removal of EVA and other polymers.

This study highlights the significant need to develop and implement eco-friendly recycling technologies in the solar industry. By advancing methods such as WGS, it is possible to recover valuable materials with high purity while minimizing their environmental impacts. These innovations can contribute to a circular economy, support sustainable development goals, and promote carbon neutrality. Future studies should optimize these processes and explore their scalability to handle the growing volume of solar panel waste effectively.

Data availability

The authors confirm that the data supporting the findings of this study are available in the article and its ESI.†

Conflicts of interest

There are no conflicts to declare.

Acknowledgements

S. H. K. and J. K. K. contributed equally to this study. This work was supported by the Korea Institute of Energy Technology Evaluation and Planning (KETEP) grant funded by the Korean Government (MOTIE) (RS-2023-0030745). It was also supported by the Korea Institute of Energy Technology Evaluation and Planning (KETEP) grant funded by the Korean Government (MOTIE) (20223030010250).

References

1 L. Chen, G. Msigwa, M. Yang, A. I. Osman, S. Fawzy, D. W. Rooney and P.-S. Yap, *Environ. Chem. Lett.*, 2022, **20**, 2277–2310.
2 J. H. Williams, R. A. Jones, B. Haley, G. Kwok, J. Hargreaves, J. Farbes and M. S. Torn, *AGU Adv.*, 2021, **2**, e2020AV000284.
3 A. Huovila, H. Siikavirta, C. A. Rozado, J. Rökman, P. Tuominen, S. Paiho, Å. Hedman and P. Ylén, *J. Cleaner Prod.*, 2022, **341**, 130912.
4 M. Madaleno, E. Dogan and D. Taskin, *Energy Econ.*, 2022, **109**, 105945.
5 J. Hu, M. Hu and H. Zhang, *Environ. Technol. Innovation*, 2023, **29**, 102960.
6 E. Mazur-Wierzbicka, *Environ. Sci. Eur.*, 2021, **33**, 1–15.
7 H. Corvellec, A. F. Stowell and N. Johansson, *J. Ind. Ecol.*, 2022, **26**, 421–432.
8 O. E. Ogunmakinde, T. Egbelakin and W. Sher, *Resour. Conserv. Recycl.*, 2022, **178**, 106023.
9 A. Qazi, F. Hussain, N. A. Rahim, G. Hardaker, D. Alghazzawi, K. Shaban and K. Haruna, *IEEE Access*, 2019, **7**, 63837–63851.
10 A. A. Kebede, T. Kalogiannis, J. Van Mierlo and M. Berecibar, *Renewable Sustainable Energy Rev.*, 2022, **159**, 112213.
11 A. Mishra and P. Bäuerle, *Angew. Chem., Int. Ed.*, 2012, **51**, 2020–2067.
12 N.-G. Park, M. Grätzel, T. Miyasaka, K. Zhu and K. Emery, *Nat. Energy*, 2016, **1**, 1–8.
13 N. S. Lewis, *Science*, 2016, **351**, aad1920.
14 T. T. Chow, A review on photovoltaic/thermal hybrid solar technology, *Renewable Energy*, 2018.
15 D. Balsalobre-Lorente, M. Shahbaz, D. Roubaud and S. Farhani, *Energy Policy*, 2018, **113**, 356–367.
16 V. Monier and M. Hestin, *Study on Photovoltaic Panels Supplementing the Impact Assessment for a Recast of the WEEE Directive*, Final Report, 2011, vol. 6.
17 R. Wang, E. Song, C. Zhang, X. Zhuang, E. Ma, J. Bai, W. Yuan and J. Wang, *RSC Adv.*, 2019, **9**, 18115–18123.
18 V. Fiandra, L. Sannino, C. Andreozzi, F. Corcelli and G. Graditi, *Waste Manage.*, 2019, **87**, 97–107.
19 J. Park and N. Park, *RSC Adv.*, 2014, **4**, 34823–34829.
20 J. Shin, J. Park and N. Park, *Sol. Energy Mater. Sol. Cells*, 2017, **162**, 1–6.

21 J. Park, W. Kim, N. Cho, H. Lee and N. Park, *Green Chem.*, 2016, **18**, 1706–1714.
22 G. Granata, F. Pagnanelli, E. Moscardini, T. Havlik and L. Toro, *Sol. Energy Mater. Sol. Cells*, 2014, **123**, 239–248.
23 F. Pagnanelli, E. Moscardini, G. Granata, T. A. Atia, P. Altimari, T. Havlik and L. Toro, *Waste Manage.*, 2017, **59**, 422–431.
24 Y. Xu, J. Li, Q. Tan, A. L. Peters and C. Yang, *Waste Manage.*, 2018, **75**, 450–458.
25 M. S. Chowdhury, K. S. Rahman, T. Chowdhury, N. Nuthammachot, K. Techato, M. Akhtaruzzaman, S. K. Tiong, K. Sopian and N. Amin, *Energy Strategy Rev.*, 2020, **27**, 100431.
26 Y.-S. Kim, A.-R. Kim, S. J. Tark, C.-B. Mo, S. Hwang and Y. Kang, *Results Eng.*, 2024, **21**, 101649.
27 N. Kyranaki, L. Perrin, L. Flandin, E. Planès, C. Farha, L. Wagner, K. Saddedine, D. Martineau and S. Cros, *Processes*, 2023, **11**, 2742.
28 S. Kashyap, J. Madan, R. Pandey and R. Sharma, Comprehensive study on the recent development of PERC solar cell, *47th IEEE Photovoltaic Specialists Conference (PVSC)*, IEEE, 2020, pp. 2542–2546.
29 M. Taguchi, *ECS J. Solid State Sci. Technol.*, 2021, **10**, 025002.
30 Y. Kim and J. Lee, *Sol. Energy Mater. Sol. Cells*, 2012, **98**, 317–322.
31 T. Doi, I. Tsuda, H. Unagida, A. Murata, K. Sakuta and K. Kurokawa, *Sol. Energy Mater. Sol. Cells*, 2001, **67**, 397–403.
32 E. Klugmann-Radziemska, P. Ostrowski, K. Drabczyk, P. Panek and M. Szkodo, *Sol. Energy Mater. Sol. Cells*, 2010, **94**, 2275–2282.
33 A. Doni and F. Dughiero, Electrothermal heating process applied to c-Si PV recycling, *38th IEEE Photovoltaic Specialists Conference*, IEEE, 2012, pp. 000757–000762.
34 L. Frisson, K. Lieten, T. Bruton, K. Declercq, J. Szlufcik, H. De Moor, M. Gorts, A. Benali and O. Aceves, Recent improvements in industrial PV module recycling, *6th European Photovoltaic Solar Energy Conference*, 2020, pp. 2160–2163.
35 B. Zhao, T. J. Kolibaba, S. Lazar and J. C. Grunlan, *Cellulose*, 2020, **27**, 4123–4132.
36 P. Wagh, R. Kumar, R. Patel, I. Singh, S. Ingale, S. C. Gupta, D. Mahadik and A. V. Rao, *J. Chem., Biol. Phys. Sci.*, 2015, **5**, 2350.
37 C. J. King, *Separation Processes*, Courier Corporation, 2013.
38 S. Haddadi, E. Ghorbel and N. Laradi, *Constr. Build. Mater.*, 2008, **22**, 1212–1219.
39 N. A. Sani, A. K. Abdulsalam and U. A. Abdullahi, *Eur. Sci. J.*, 2013, **9**, 160–168.
40 W.-J. Lee and Y.-H. Chang, *Coatings*, 2018, **8**, 431.